

## Mechanistic Insight on the Hydrogenation of Conjugated Alkenes with H<sub>2</sub> Catalyzed by Early Main-Group Metal Catalysts

Guixiang Zeng and Shuhua Li\*

*School of Chemistry and Chemical Engineering, Key Laboratory of Mesoscopic Chemistry of Ministry of Education, Institute of Theoretical and Computational Chemistry, Nanjing University, Nanjing 210093, P. R. China*

Received December 5, 2009

Density functional theory calculations have been performed to investigate the molecular mechanism of the hydrogenation reactions of 1,1-diphenylethylene and myrcene catalyzed by the actual calcium hydride catalyst, CaH(dipp-nacnac)(thf) (dipp-nacnac = CH{(CMe)(2,6-iPr<sub>2</sub>-C<sub>6</sub>H<sub>3</sub>N)}<sub>2</sub>). The hydrogenation reactions of these two alkenes proceed via a similar pathway, which includes three steps. First, the hydride migrates from the calcium center to one olefinic carbon in the substrate. Then, the hydride transfer product can easily transform into a key ion-pair intermediate. This intermediate provides an intramolecular frustrated Lewis pair, in which the calcium center acts as a Lewis acid, and one olefinic carbon acts as a Lewis base. Next, the H–H bond is heterolytically cleaved by this frustrated Lewis pair through a concerted Lewis acid–Lewis base mechanism, producing the hydrogenation product and regenerating the catalyst. For these two reactions, the rate-limiting step is the hydride transfer step, with free energy barriers of 29.2 kcal for both substrates. In addition, our calculations indicate that the hydrogenation reaction of 1,1-diphenylethylene catalyzed by the analogous strontium hydride complex may readily occur, but the similar magnesium-mediated hydrogenation reaction is less likely to take place under similar conditions as adopted by the calcium hydride catalyst. The results can give satisfactory descriptions of experimental facts observed for these two hydrogenation reactions. The hydrogenation mechanism proposed here is different from that of the late transition metal-catalyzed alkene hydrogenation or the organolanthanide-catalyzed alkene hydrogenation.

### 1. Introduction

The catalytic hydrogenation of unsaturated compounds is widely used in numerous industrial processes.<sup>1</sup> For example, it is a key step in the synthesis of fine chemicals<sup>2–5</sup> as well as pharmaceutical compounds.<sup>6–10</sup> Traditionally, most homogeneous hydrogenations are catalyzed by the noble transition metals,

such as Pd,<sup>11,12</sup> Ru,<sup>13–18</sup> and Rh.<sup>19–25</sup> The hydrogenation process usually includes the following steps (as shown in Scheme 1): (1) the oxidative addition of dihydrogen to the metal, (2) coordination of the unsaturated substrate to the metal, (3) insertion of the coordinated substrate to the M–H

\*To whom correspondence should be addressed. E-mail: shuhua@nju.edu.cn.

(1) Bartok, M.; Felföldi, K. *Stereochemistry of Heterogeneous Metal Catalysis*; Wiley: Chichester, U. K., 1985; Chapter VII.

(2) Blaser, H.-U.; Malan, C.; Pugin, B.; Spindler, F.; Steiner, H.; Studer, M. *Adv. Synth. Catal.* **2003**, *345*, 103–151.

(3) Saudan, L. A. *Acc. Chem. Res.* **2007**, *40*, 1309–1319.

(4) Torres, G. C.; Ledesma, S. D.; Jablonski, E. L.; Miguel, S. R. D.; Scelza, O. A. *Catal. Today* **1999**, *48*, 65–72.

(5) Tadepalli, S.; Qian, D.; Lawal, A. *Catal. Today* **2007**, *125*, 64–73.

(6) Koo-amornpattana, W.; Winterbottom, J. M. *Catal. Today* **2001**, *66*, 277–287.

(7) Knowles, W. S. *Adv. Synth. Catal.* **2003**, *345*, 3–13.

(8) Alsten, J. G. V.; Jorgensen, M. L.; Ende, D. J. A. *Org. Proc. Res. Dev.* **2009**, *13*, 629–633.

(9) Johnson, N. B.; Lennon, I. C.; Moran, P. H.; Ramsden, J. A. *Acc. Chem. Res.* **2007**, *40*, 1291–1299.

(10) Lennon, I. C.; Pilkington, C. J. *Synthesis—Stuttgart* **2003**, *11*, 1639–1642.

(11) Pham-Huu, C.; Keller, N.; Charbonniere, L. J.; Ziesel, R.; Ledoux, M. J. *Chem. Commun.* **2000**, 1871–1872.

(12) Mori, S.; Ohkubo, T.; Ikawa, T.; Kume, A.; Maegawa, T.; Monoguchi, Y.; Sajiki, H. *J. Mol. Catal. A: Chem.* **2009**, *307*, 77–87.

(13) Claver, C.; Fernandez, E.; Gillon, A.; Hyett, D. J.; Orpen, A. G.; Pringle, P. G. *Chem. Commun.* **2000**, *11*, 961–962.

(14) Abdur-Rashid, K.; Lough, A. J.; Morris, R. H. *Organometallics* **2000**, *19*, 2655–2657.

(15) Ohkuma, T.; Koizumi, M.; Muñiz, K.; Hilt, G.; Kabuto, C.; Noyori, R. *J. Am. Chem. Soc.* **2002**, *124*, 6508–6509.

(16) Evans, D. A.; Michael, F. E.; Tedrow, J. S.; Campos, K. R. *J. Am. Chem. Soc.* **2003**, *125*, 3534–3543.

(17) Schrockla, R. R.; Osborn, J. A. *J. Am. Chem. Soc.* **1976**, *98*, 8265–8266.

(18) Hannedouche, J.; Clarkson, G. J.; Wills, M. *J. Am. Chem. Soc.* **2004**, *126*, 986–987.

(19) Yang, H.; Gao, H.; Angelici, R. J. *Organometallics* **2000**, *19*, 622–629.

(20) Abdur-Rashid, K.; Lough, A. J.; Morris, R. H. *Organometallics* **2001**, *20*, 1047–1049.

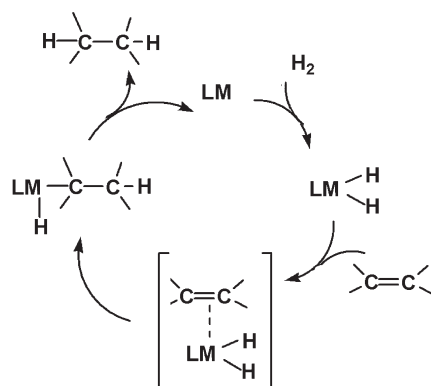
(21) Burk, M. J.; Hems, W.; Herzberg, D.; Malan, C.; Zanotti-Gerosa, A. *Org. Lett.* **2000**, *2*, 4173–4176.

(22) Hannedouche, J.; Clarkson, G. J.; Wills, M. *J. Am. Chem. Soc.* **2004**, *126*, 986–987.

(23) Ohkuma, T.; Koizumi, M.; Muñiz, K.; Hilt, G.; Kabuto, C.; Noyori, R. *J. Am. Chem. Soc.* **2002**, *124*, 6508–6509.

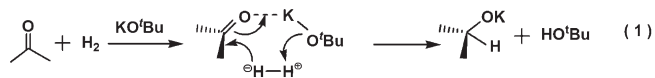
(24) Ito, M.; Ikariya, T. *Chem. Commun.* **2007**, *48*, 5134–5142.

(25) Casey, C. P.; Singer, S. W.; Powell, D. R.; Hayashi, R. K.; Kavana, M. *J. Am. Chem. Soc.* **2001**, *123*, 1090–1100.

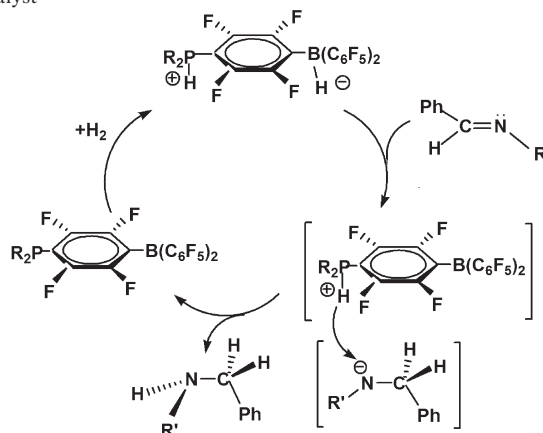
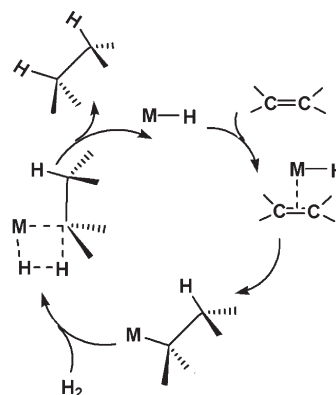
**Scheme 1.** Hydrogenation Mechanism Catalyzed by the Transition Metal Complex

bond, and (4) reductive elimination to produce the final product. However, in catalytic ionic hydrogenation based on inexpensive metals (such as W and Mo),<sup>26</sup> the reaction usually starts by proton transfer from a cationic metal dihydride to the unsaturated substrate, then the metal-bound hydride transfers to the protonated substrate to generate the product.

In recent years, new-generation hydrogenation catalysts have been pursued in order to reduce the cost of the catalysts and make the catalytic processes environmentally friendly. New hydrogenation catalysts can be divided into two categories. (1) Nontransition-metal catalysts: for example, in 2002, Müller et al found that the hydrogenation of ketones can occur with KO<sup>t</sup>Bu as the catalyst under mild conditions (eq 1).<sup>27,28</sup> (2) Metal-free catalysts: in 2007, Stephen et al first reported hydrogenations of imines and ketone catalyzed by phosphine–borane species (Scheme 2).<sup>29,30</sup> The latter reaction is based on the concerted H–H splitting catalyzed by frustrated Lewis pairs.<sup>31–36</sup>



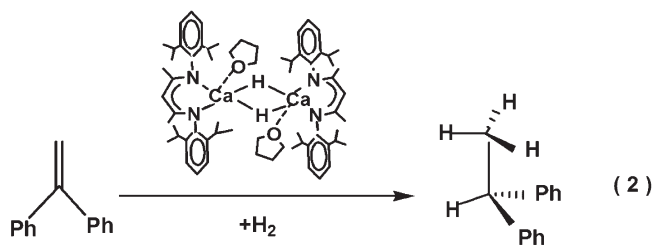
However, main-group metal catalysts for the hydrogenation of alkenes with H<sub>2</sub> are still rarely known. In some hydrogenation reactions, main-group metal complexes such as LiAlH<sub>4</sub> or KH are involved, but these reactions require harsh conditions and various products are obtained.<sup>37,38</sup> In

**Scheme 2.** Hydrogenation of Imines Catalyzed by the Metal-Free Catalyst**Scheme 3.** Mechanism for Organolanthanide-Catalyzed Alkene Hydrogenation

2008, Harder and his co-workers reported well-defined organocalcium catalysts, which can catalyze the hydrogenation of a variety of conjugated alkenes with H<sub>2</sub> under mild conditions (eq 2).<sup>39</sup> In their experiments, several organocalcium catalysts were found to be effective. For example, the hydrogenation of 1,1-diphenylethylene (DPE) can occur at 60 °C, in the presence of the well-defined catalyst {CaH(dipp-nacnac)(thf)}<sub>2</sub> (dipp-nacnac = CH{(CMe)(2,6-*i*Pr<sub>2</sub>-C<sub>6</sub>H<sub>3</sub>N)}<sub>2</sub>). To explain the observed experimental facts, the authors proposed that the hydrogenation mechanism is analogous to that for organolanthanide-catalyzed alkene hydrogenation, as shown in Scheme 3.<sup>40</sup> In this mechanism, the substrate (alkene) inserts into the M–H bond followed by the calcium–carbon bond formation. Next, H<sub>2</sub> is added to the calcium–carbon bond to generate the saturated product and recover the catalyst via a “four-center” transition state. It should be mentioned that, in the crystal structure of one of the intermediates characterized experimentally, the calcium atom is coordinated to one of the phenyl ring rather than one carbon atom of the ethylene component. This intermediate does not appear in the reaction pathway suggested above. In addition, it is not clear why these organocalcium catalysts (or its strontium analogous) can only catalyze the hydrogenation of substrates with conjugated double bonds. Therefore, a detailed computation study on

(26) Bullock, R. M. *Chem.—Eur. J.* **2004**, *10*, 2366–2374.(27) Berkessel, A.; Schubert, T. J. S.; Müller, T. N. *J. Am. Chem. Soc.* **2002**, *124*, 8693–8698.(28) Chan, B.; Radom, L. *J. Am. Chem. Soc.* **2005**, *127*, 2443–2454.(29) Sumerin, V.; Schulz, F.; Nieger, M.; Leskelä, M.; Repo, T.; Rieger, B. *Angew. Chem., Int. Ed.* **2008**, *47*, 6001–6003. *Angew. Chem.* **2008**, *120*, 6090–6092.(30) Chase, P. A.; Welch, C. G.; Jurca, T.; Stephan, D. W. *Angew. Chem., Int. Ed.* **2007**, *46*, 8050–8053. *Angew. Chem.* **2007**, *119*, 8196–8199.(31) Guo, Y.; Li, S. *Inorg. Chem.* **2008**, *47*, 6212–6219.(32) Chase, P. A.; Jurca, T.; Stephan, D. W. *Chem. Commun.* **2008**, *14*, 1701–1703.(33) Rokob, T. A.; Hamza, A.; Stirling, A.; Soós, T.; Pápai, I. *Angew. Chem., Int. Ed.* **2008**, *47*, 2435–2438. *Angew. Chem.* **2008**, *120*, 2469–2472.(34) Rokob, T. A.; Hamza, A.; Stirling, A.; Pápai, I. *J. Am. Chem. Soc.* **2009**, *131*, 2029–2036.(35) Rokob, T. A.; Hamza, A.; Pápai, I. *J. Am. Chem. Soc.* **2009**, *131*, 10701–10710.(36) Hamza, A.; Stirling, A.; Rokob, T. A.; Pápai, I. *Int. J. Quant. Chem.* **2009**, *109*, 2416–2425.(37) Slaugh, L. H. *Tetrahedron* **1966**, *22*, 1741–1746.(38) Slaugh, L. H. *J. Org. Chem.* **1967**, *32*, 108–113.(39) Spielmann, J.; Buch, F.; Harder, S. *Angew. Chem., Int. Ed.* **2008**, *47*, 9434–9438. *Angew. Chem.* **2008**, *120*, 9576–9580.(40) Jeske, G.; Lauke, H.; Mauermann, H.; Schumann, H.; Marks, T. J. *J. Am. Chem. Soc.* **1985**, *107*, 8111–8118.

the molecular mechanism of the calcium-mediated hydrogenation of conjugated alkenes described above is still desirable. Understanding the mechanism of this type of reaction at the molecular level will provide important information for the design of more effective main-group metal-based catalysts for alkene hydrogenation. In this work, we have performed detailed density functional theory (DFT) calculations to investigate the molecular mechanism for two typical hydrogenation reactions catalyzed by  $\{CaH(dipp-nacnac)(thf)\}_2$ , the hydrogenation reactions of DPE and myrcene, respectively. These two substrates can be considered as two typical examples of conjugated alkenes. In addition, we have also investigated the catalytic behaviors of the analogous organomagnesium and organostrontium catalysts for the hydrogenation reaction of DPE.



## 2. Computational Details

All the species were fully optimized using the Gaussian03 program<sup>41</sup> with the B3LYP hybrid functional.<sup>42,43</sup> For Ca and Mg, the 6-311++G(d,p) basis set was employed, and for Sr, the effective core potential LANL2DZ<sup>44</sup> and a modified LANL2DZ basis set with optimized 5p functions<sup>45</sup> and a set of f-type functions was used.<sup>46</sup> For the reaction of DPE, the 6-31G basis set was used for atoms outside the active center, which include two methyl groups and two 2,6-diisopropylphenyl groups, the tetrahydrofuran (thf) ligand (except the oxygen atom), and one phenyl group (except the carbon atom bonded to the double bond). For all the other atoms, the 6-311++G(d,p) basis set was used. For the substrate myrcene, the 6-311++G(d,p) basis set was employed for the butadiene component and the 6-31G basis set was used for other atoms. For each stationary point on the potential energy surface, a frequency calculation was carried out to make sure whether it is a minimum or a transition state, and

to obtain its gas-phase Gibbs free energy. In addition, all the transition states were verified by intrinsic reaction coordinate (IRC)<sup>47</sup> calculations. The polarizable-continuum model (PCM)<sup>48</sup> was employed to compute the solvation Gibbs free energy for each species at its gas-phase optimized structure. For each species in the solvent (benzene), its free energy is evaluated as the sum of its gas-phase free energy (obtained at a given temperature and pressure) and the solvation free energy.

## 3. Results and Discussions

In this section, the generation of the actual catalyst is discussed first. Then, results on the hydrogenation reactions of DPE and myrcene catalyzed by the calcium hydride complex will be discussed, respectively. In the last subsection, we explore the free energy profiles of the hydrogenation of DPE catalyzed by the analogous magnesium-hydride and strontium-hydride catalysts.

**3.1. Active Form of the Calcium Catalyst.** The calcium catalyst,  $\{CaH(dipp-nacnac)(thf)\}_2$ , is a dimeric species, as shown by its crystal structure.<sup>49</sup> However, the crystal structure of the hydride transfer intermediate suggests that only its monomer is involved in the reaction. Thus, it is worthwhile to investigate the energetics of the dissociation process of the dimeric species into two monomers. We have optimized the structures of the dimer and its corresponding monomer, the calcium hydride complex (CaH(dipp-nacnac)(thf), species **1** in Figure 1). The optimized structural parameters of the dimer (as shown in Figure S1, Supporting Information) are in very good agreement with those of the crystal structure. The dissociation free energy from the dimer to two monomers is calculated to be 13.3 kcal/mol in the gas phase (60 °C and 20 bar) and  $-7.7$  kcal/mol in the solvent (benzene). Thus, it is very likely for the calcium catalyst,  $\{CaH(dipp-nacnac)(thf)\}_2$ , to decompose into two calcium hydride complexes. On the basis of the experimental results and calculated results described above, we assume that the active form of the calcium catalyst would be the calcium hydride complex.

**3.2. The Calcium-Mediated Hydrogenation Reaction of DPE.** For this reaction, we have located all possible intermediates and transition states which may be involved. The optimized structures of these stationary points are displayed in Figure 1. The Gibbs free energy profiles calculated in gas phase (60 °C and 20 bar) and in the solvent are presented in Figure 2. In the following discussion, free energies obtained in the solvent will be used exclusively in discussing the reaction pathway.

In the active catalyst **1**, the Ca–H1 distance is 2.073 Å. The natural atomic charges on Ca and H1 are 1.71e and  $-0.82e$ , respectively, an indication that H1 is hydridic. For the substrate **2** (DPE), the C1=C2 bond length is 1.343 Å. The C2–C3 distance is 1.490 Å, being close to a typical single C–C bond rather than a typical C=C bond.

First, the hydride H1 migrates from the calcium center in **1** to the terminal carbon (C1) of the double bond in the substrate **2** via the transition state TS<sub>1</sub>. In TS<sub>1</sub>, the distances of Ca–H1 and H1–C1 are 2.169 and 1.647 Å, respectively. The activation free energy of this step is 29.2 kcal/mol. About the ion-pair product from this hydride

(41) Frisch, M. J.; Trucks, G. W.; Schlegel, H. B.; Scuseria, G. E.; Robb, M. A.; Cheeseman, J. R.; Montgomery, J. A., Jr.; Vreven, T.; Kudin, K. N.; Burant, J. C.; Millam, J. M.; Iyengar, S. S.; Tomasi, J.; Barone, V.; Mennucci, B.; Cossi, M.; Scalmani, G.; Rega, N.; Petersson, G. A.; Nakatsuji, H.; Hada, M.; Ehara, M.; Toyota, K.; Fukuda, R.; Hasegawa, J.; Ishida, M.; Nakajima, T.; Honda, Y.; Kitao, O.; Nakai, H.; Klene, M.; Li, X.; Knox, J. E.; Hratchian, H. P.; Cross, J. B.; Adamo, C.; Jaramillo, J.; Gomperts, R.; Stratmann, R. E.; Yazyev, O.; Austin, A. J.; Cammi, R.; Pomelli, C.; Ochterski, J. W.; Ayala, P. Y.; Morokuma, K.; Voth, G. A.; Salvador, P.; Dannenberg, J. J.; Zakrzewski, V. G.; Dapprich, S.; Daniels, A. D.; Strain, M. C.; Farkas, O.; Malick, D. K.; Rabuck, A. D.; Raghavachari, K.; Foresman, J. B.; Ortiz, J. V.; Cui, Q.; Baboul, A. G.; Clifford, S.; Cioslowski, J.; Stefanov, B. B.; Liu, G.; Liashenko, A.; Piskorz, P.; Komaromi, I.; Martin, R. L.; Fox, D. J.; Keith, T.; Al-Laham, M. A.; Peng, C. Y.; Nanayakkara, A.; Challacombe, M.; Gill, P. M. W.; Johnson, B.; Chen, W.; Wong, M. W.; Gonzalez, C.; Pople, J. A. A. *Gaussian 03*, revision B.04; Gaussian Inc.: Wallingford, CT, 2004.

(42) Becke, A. D. *J. Chem. Phys.* **1993**, *98*, 5648–5652.

(43) Lee, C.; Yang, W.; Parr, R. G. *Phys. Rev. B* **1988**, *37*, 785–789.

(44) Hay, P. J.; Wadt, W. R. *J. Chem. Phys.* **1985**, *82*, 299–310.

(45) Couty, M.; Hall, M. B. *J. Comput. Chem.* **1996**, *17*, 1359–1370.

(46) Ehler, A. W.; Böhme, M.; Dapprich, S.; Gobbi, A.; Höllwarth, A.; Jonas, V.; Köhler, K. F.; Segmann, R.; Velkamp, A.; Frenking, G. *Chem. Phys. Lett.* **1993**, *208*, 111–114.

(47) Gonzalez, C.; Schlegel, H. B. *J. Chem. Phys.* **1989**, *90*, 2154–2161.

(48) Tomasi, J.; Persico, M. *Chem. Rev.* **1994**, *94*, 2027–2094.

(49) Spielmann, J.; Harder, S. *Chem.—Eur. J.* **2008**, *14*, 1480–1486.

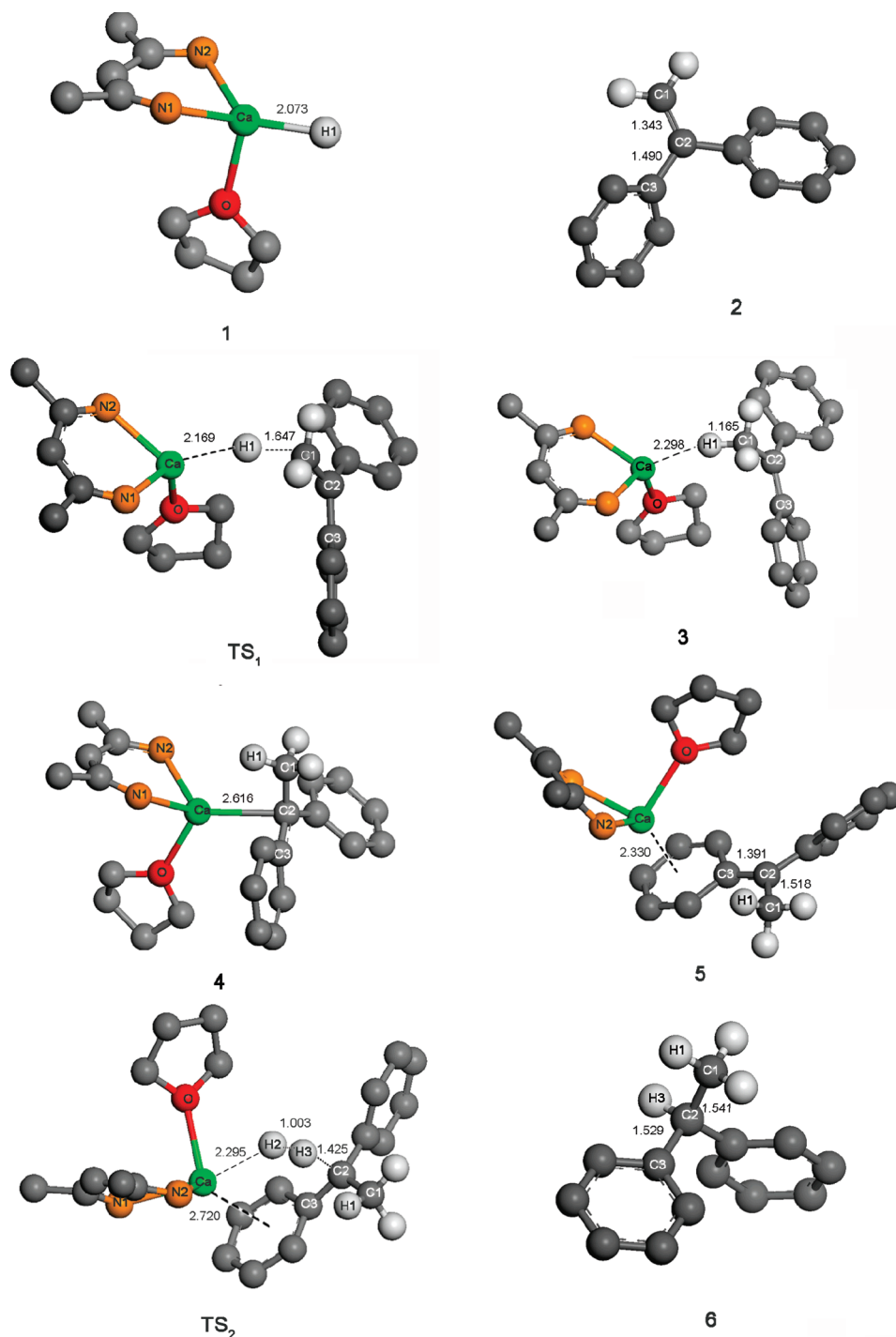


**Figure 1.** Optimized structures of all the stationary points involved in the calcium-mediated hydrogenation of DPE. All hydrogen atoms (except those involved in the hydrogenation reaction) and two 2,6-diisopropylphenyl substituents bound to the nitrogen atoms are omitted for clarity. All the distances are in Å.

transfer, we found it is difficult to locate its structure. This is because, after the terminal carbon (C1) accepts the hydride H1, the Ca(dipp-nacnac)(thf) component becomes a singly charged cation, and the substrate component becomes a singly charged anion,  $(\text{Ph}_2\text{CMe})^-$ . We have made many attempts to find this ion-pair product. First, we have performed IRC calculations, with the results shown in Figure S2 (Supporting Information). Along one direction, the reaction path readily goes to the reactants **1** and **2**, and along another direction, the reaction path goes toward the expected ion-pair product.

However, IRC calculations abnormally terminated at a given structure, in which the distances of Ca–H1 and H1–C1 are 2.488 and 1.219 Å, respectively, and the three atoms (Ca, H1, C1) are almost in a linear arrangement. Then, starting from this initial structure, we located a product-like structure, **3**. This structure can be obtained when loose optimization convergence criteria are employed, possibly due to the very flat potential energy surface near this structure. If optimization convergence criteria are tightened, all geometry optimizations eventually lead to the species **5**. In species **3**, the Ca–H1 and

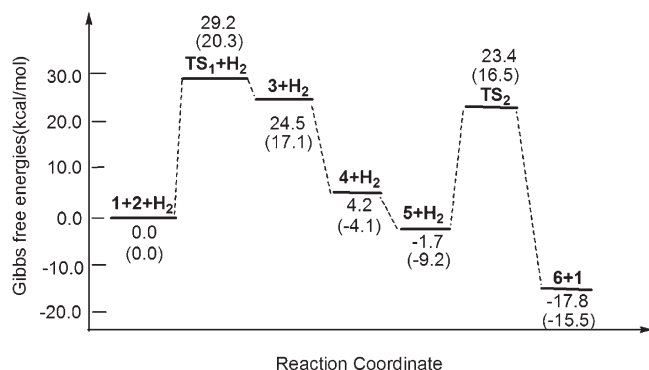


**Figure 2.** Gibbs free energy profile of the calcium-mediated hydrogenation of DPE with H<sub>2</sub> in the solvent. The corresponding free energies in gas phase (60 °C and 20 bar) are also presented in parentheses for comparison.

H1–C1 distances are 2.298 and 1.165 Å, respectively, and the angle ∠Ca–H1–C1 is 162°. Thus, the hydride transfer is completed in **3**.

As mentioned above, the potential energy surface around **3** is very flat, indicating that the ion-pair complex **3** should have a very flexible structure.<sup>49</sup> Thus, species **3** could easily transform into more stable species. For example, the calcium center could bind to the disubstituted carbon of the double bond to form species **4**, which is 20.3 kcal/mol lower in free energy than **3**, or it may coordinate to one of the phenyl ring, generating an even more stable species **5**.

It is difficult to locate the transition state from **3** to **4**. However, by constraining ∠Ca–C3–C2 at several values and optimizing all other degrees of freedom, one can obtain an approximate potential energy surface (as shown in Figure S3, Supporting Information) for the transformation from **3** to **4**. It turns out that this step is almost barrierless.

In species **4**, the Ca–C3 bond distance is 2.616 Å, indicating a strong steric repulsion between large groups in DPE and the dipp-nacnac ligand. However, species **4** is less stable than **5** by 5.9 kcal/mol in Gibbs free energy. Thus, the calcium center could shift slightly toward the center of one of the phenyl rings to form the more stable intermediate **5**. We have carried out a relaxed potential energy surface scan by fixing ∠Ca–C3–C2 at a series of values to probe the possible energy barrier from **4** to **5**, with the results shown in Figure S4 (Supporting Information). It can be seen that the electronic energy barrier is about 1.0 kcal/mol, which indicates that the transformation from **4** to **5** can occur readily. This result is in accord with the fact that species **5** was detected experimentally.

For **5**, its optimized structural parameters are in good agreement with the X-ray crystal structure (Figure S5, Supporting Information).<sup>39</sup> The C1–C2 and C2–C3 distances are 1.518 and 1.391 Å, respectively, being close to the corresponding experimental bond lengths (1.521 and 1.387 Å). The double bond character of the C2–C3 bond induces charge delocalization in the ring. The natural atomic charges are 1.82e on Ca, –0.62e in the ring bound to Ca, and –0.19e on C2. Thus, the electrostatic interaction between the calcium center and the phenyl ring is the main driving force for forming complex

**Table 1.** Natural Atomic Charges on Atoms Involved in the Calcium-Mediated H–H Cleavage Process of DPE (TS<sub>2</sub> is the Transition State, **1** and **6** are the Products)

	<b>5</b>	TS <sub>2</sub>	<b>1</b>	<b>6</b>
Ca	1.82	1.80	1.71	
H2		–0.43	–0.82	
H3		0.19		0.21
C2	–0.19	–0.39		–0.25

**5**. The calcium complexes with a Ph···Ca electrostatic interaction are ubiquitous in biological systems.<sup>50–54</sup>

In **5**, the distance between the calcium center and C2 is 4.010 Å. The atomic charges on these two atoms show that Ca is a Lewis acid, and C2 is a Lewis base. Thus, this structure can be considered an intramolecular frustrated Lewis pair, which can heterolytically split the H–H bond under mild conditions through a concerted Lewis acid–Lewis base mechanism.<sup>31–36</sup> This viewpoint is confirmed by our calculations. The corresponding transition state (TS<sub>2</sub>) for the activation of H<sub>2</sub> has been successfully located. In TS<sub>2</sub>, the Ca–H2, H<sub>2</sub>–H3, and H3–C2 distances are 2.295, 1.003, and 1.425 Å, respectively. At the same time, the C1–C2 and C2–C3 bonds are elongated from 1.518 and 1.391 Å in **5** to 1.526 and 1.446 Å in TS<sub>2</sub>. As shown in Table 1, the natural atomic charges are –0.43e on H2 and 0.19e on H3 in TS<sub>2</sub>, indicating that the H–H bond is heterolytically cleaved by the cooperation of the calcium center and the benzylic C2 atom. This mechanism is very similar to that shown in metal-free catalysts.<sup>31–36</sup> The free energy barrier of this step is 25.1 kcal/mol. After the H–H bond is cleaved, the catalyst (species **1**) is regenerated and the final product **6** is produced. Our geometry optimization shows that product **6** will not bind to the calcium center.

Since species **4** is also an intermediate in the σ-bond metathesis mechanism proposed previously,<sup>55</sup> we have tried to locate the “four-center” transition state for H<sub>2</sub> activation. However, our geometry optimizations show that such a transition state does not exist on the potential energy surface. Thus, the reaction is unlikely to proceed via the σ-bond metathesis mechanism.

To conclude, under experimental conditions (60 °C and 20 bar), the overall reaction is exothermic by 17.8 kcal/mol in the solvent, and the rate-limiting step is the hydride transfer process with a free energy barrier of 29.2 kcal/mol. To test the influence of hydrogen pressure on the Gibbs free energy barrier, we have calculated the free energy barrier for the rate-limiting step under atmospheric pressure (1 bar). The calculated free energy barrier is 31.2 kcal/mol. Thus, higher hydrogen pressure (20 bar) would facilitate the hydride transfer process.

**3.3. The Calcium-Mediated Hydrogenation Reaction of Myrcene.** For this reaction, the optimized structures of all stationary points are presented in Figure 3, and the

(50) Song, Z.; Wang, H.; Xing, L. *J. Solution Chem.* **2009**, *38*, 1139–1154.

(51) Wall, S. L. D.; Meadows, E. S.; Barbour, L. J.; Gokel, G. W. *J. Am. Chem. Soc.* **1999**, *121*, 5613–5614.

(52) Deacon, G. B.; Forsyth, C. M.; Jaroschik, F.; Junk, P.; Kay, D. L.; Maschmeyer, T.; Masters, A. F.; Wang, J.; Field, L. *Organometallics* **2008**, *27*, 4772–4778.

(53) Kriek, S.; Görls, H.; Yu, L.; Reiher, M.; Westerhausen, M. *J. Am. Chem. Soc.* **2009**, *131*, 2977–2985.

(54) Kang, H. S. *J. Phys. Chem. A* **2005**, *109*, 1458–1467.

(55) Kaufmann, E.; Sieber, S.; Schleyer, P. v. R. *J. Am. Chem. Soc.* **1989**, *111*, 121–125.

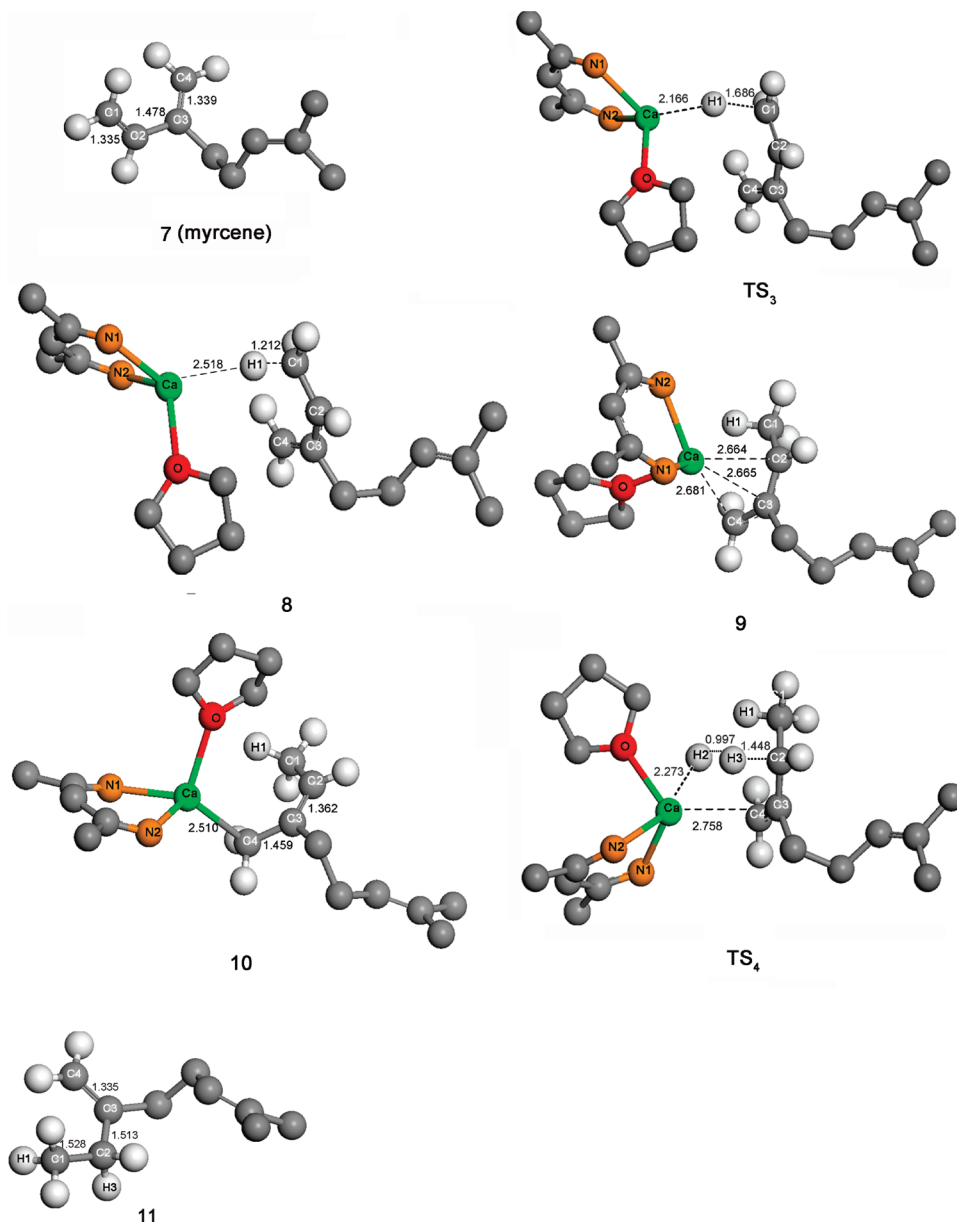


**Figure 3.** Optimized structures of all the stationary points involved in the calcium-mediated hydrogenation of myrcene. All hydrogen atoms (except those involved in the hydrogenation reaction) and two 2,6-diisopropylphenyl substituents bound to the nitrogen atoms are omitted for clarity. All the distances are in Å.

corresponding Gibbs free energy profile is shown in Figure 4. The reaction pathways of this reaction are similar to those of the hydrogenation reaction of DPE, which include two steps. First, the hydride migrates from the calcium center to one of two terminal carbon atoms of the butadiene component via the transition state  $TS_3$  to form an ion-pair intermediate **8**. Similarly, another isomer of **8** may also be produced, in which the hydride is abstracted by another terminal carbon (C4) of the butadiene component. As the ion-pair complex is expected to have a flexible structure, this intermediate, **8**, can only be approximately located by following the intrinsic reaction coordinate. From the structure of **8**, one can see that the hydride is transferred from the calcium center to the C1 atom. The free energy barrier for the hydride transfer step is 29.2 kcal/mol in the solvent.

Starting with the structure of **8**, full geometry optimizations eventually lead to a more stable species **9**. This result indicates that the rearrangement from **8** to **9**

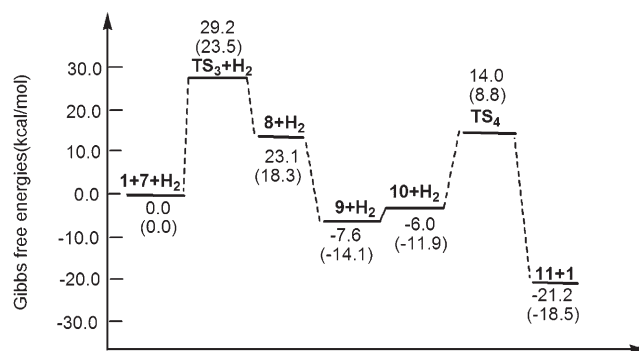


**Figure 4.** Gibbs free energy profile of the calcium-mediated hydrogenation of myrcene with  $H_2$  in the solvent. The corresponding free energies in the gas phase (60 °C and 20 bar) are also presented in parentheses for comparison.

almost barrierless. In **9**, the Ca–C2, Ca–C3, and Ca–C4 distances are 2.664, 2.665, and 2.681 Å, respectively.

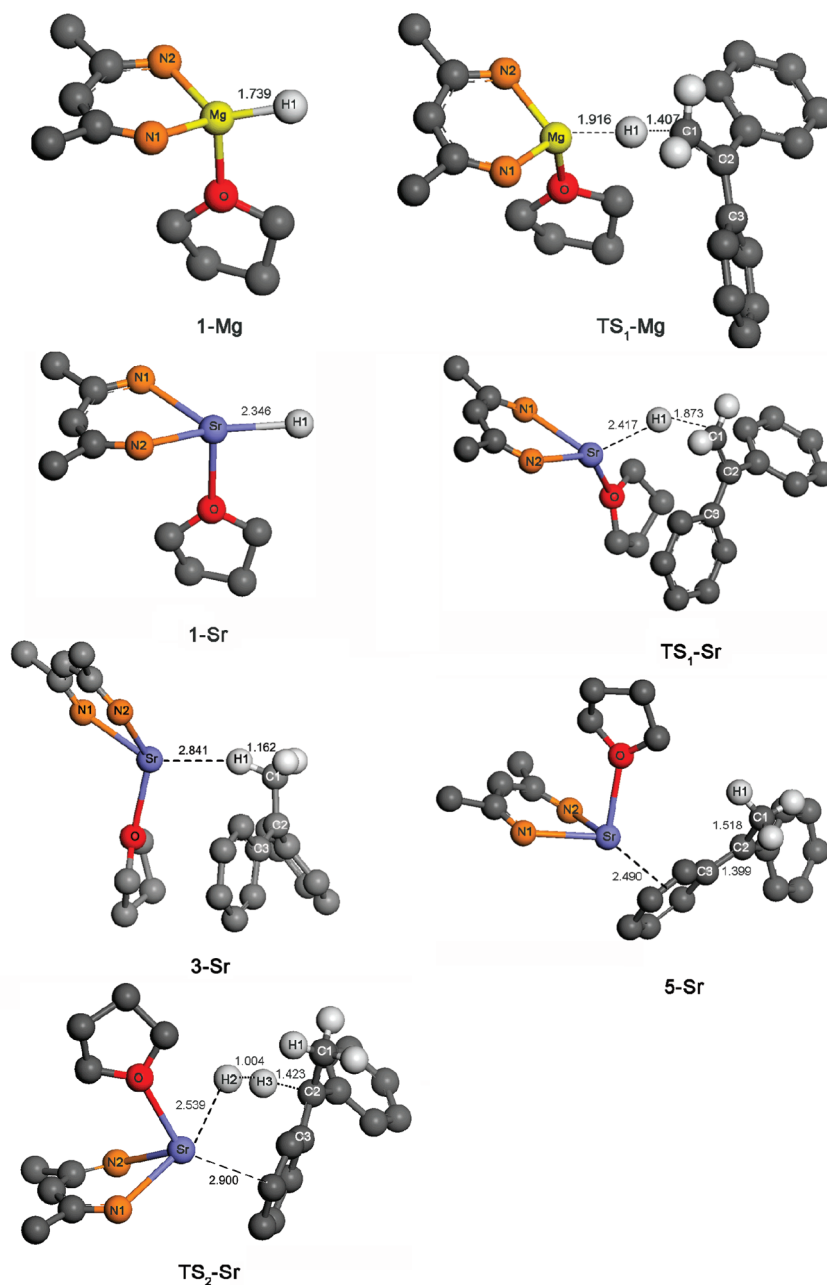


**Figure 5.** Optimized structures of some stationary points involved in the magnesium- and strontium-mediated hydrogenation reaction of DPE. All hydrogen atoms (except those involved in the hydrogenation reaction) and two 2,6-diisopropylphenyl substituents bound to the nitrogen atoms are omitted for clarity. All the distances are in Å.

Thus, the allyl group is bound to the metal in the  $\eta^3$  form. Next, this  $\eta^3$ -allyl complex **9** will have to transform into the  $\sigma$ -allyl complex **10** to facilitate the hydrogen activation. In species **10**, the C4 atom of the allyl group is bonded to the metal, and the C2–C3 bond becomes a double bond (1.362 Å). The natural atomic charges are 1.84e on Ca,  $-0.17e$  on C2, and  $-0.02e$  on C3. Thus, species **10** can also be considered as an intramolecular frustrated Lewis pair (Ca is a Lewis acid and C2 is a Lewis base). Species **10** is 1.6 kcal/mol above the  $\eta^3$ -allyl complex **9**. Our potential energy surface scan shows that the energy barrier for the transformation from **9** to **10** is very close to the energy difference between these two species. All attempts to locate the transition state between two species failed.

Next,  $H_2$  is activated by species **10** via  $TS_4$  to produce the final product **11** and regenerate the catalyst. The transition state for the heterolytic H–H bond cleavage ( $TS_4$ ) is structurally analogous to  $TS_2$  in the hydrogenation reaction of DPE. This step is strongly exothermic, with a free energy barrier of 20.0 kcal/mol with respect to **10** and  $H_2$  (or 21.6 kcal/mol relative to **9** and  $H_2$ ).

To conclude from the discussions above, the hydrogenation reaction of myrcene catalyzed by the calcium hydride complex **1** is thermodynamically favorable, and the rate-limiting step (the hydride transfer) has a free energy barrier of 29.2 kcal/mol in the solvent (benzene). These results can give satisfactory descriptions for the experimentally observed hydrogenation reaction of myrcene catalyzed by the calcium hydride complex. Experimentally, the calcium

hydride complex was found to catalyze the hydrogenation reaction of a variety of alkenes with conjugated double bonds. One can understand this fact by examining the structures of the key intermediate **5** or **10**. These two intermediates can be considered as intramolecular frustrated Lewis pairs, which can heterolytically cleave  $H_2$  under mild conditions. It should be mentioned that species **5** is the first frustrated Lewis pair characterized by X-ray diffraction until now. Clearly, the negatively charged phenyl ring is necessary for binding to the calcium cation to yield the frustrated Lewis pair **5**. In the meantime, the negatively charged allyl group is required for the formation of the key intermediate **9**, which is the precursor for the frustrated Lewis pair **10**. Thus, the existence of conjugated double bonds or phenyl rings in the substrates is essential for the formation of intramolecular frustrated Lewis pairs, which are reactive intermediates in heterolytic  $H_2$  activation.

**3.4. The Hydrogenation Reactions of DPE Catalyzed by the Magnesium or Strontium Hydride Complex.** It is interesting to investigate whether the hydrogenation reaction of DPE could also be catalyzed by the analogous magnesium or strontium hydride complex. Following a similar reaction pathway to that described above, we have optimized the structures of some stationary points for the magnesium-mediated and strontium-mediated hydrogenation reactions, which are displayed in Figure 5.

For the hydride transfer step, the free energy barrier from the reactants (the catalyst and the substrate) to the transition state is calculated to be 34.3 kcal/mol for the magnesium hydride catalyst and 27.6 kcal/mol for the strontium hydride catalyst, respectively. Thus, under similar conditions as required by the calcium hydride complex, the hydride transfer step from the magnesium hydride complex to the substrate is difficult to take place, while this step can occur readily for the strontium hydride complex. As a result, the hydrogenation of DPE catalyzed by the magnesium hydride catalyst is less likely to occur.

For the strontium-mediated reaction, we have also explored the potential energy profile of the following steps, and the free energy profiles of all steps are presented in Figure 6. For the hydride transfer product **3-Sr**, its structure was approximately located as in locating species **8**. In **3-Sr**, the distances of Sr–H1 and H1–C1 are 2.841 and 1.162 Å, respectively. Surprisingly, we failed to locate the expected **4-Sr** (structurally similar to **4**), possibly because Sr has a much larger atomic radius than Ca. Full geometry optimizations with the expected **4-Sr** as the initial structure always result in the more stable ion-pair complex **5-Sr**. In **5-Sr**, the distance between the Sr atom and the benzylic C2 atom is 3.860 Å, which is shorter than that (4.010 Å) in species **5**. The natural atomic charges on Sr (1.90e) and C2 (–0.21e) in **5-Sr** are slightly larger than those in its analog **5**. This result indicates that **5-Sr** might split the H–H bond more easily than species **5**. Our calculations have confirmed this viewpoint. The transition state (**TS<sub>2</sub>-Sr**) for the H–H bond cleavage is only 13.9 kcal/mol in free energy above the **5-Sr** complex and  $H_2$ . For the overall reaction, the rate-limiting step is the hydride transfer step with a barrier of 27.6 kcal/mol in the solvent. Thus, our calculations demonstrate that the strontium hydride catalyst should have similar catalytic behaviors for the hydrogenation reaction of DPE like its calcium hydride analog. Experimentally,

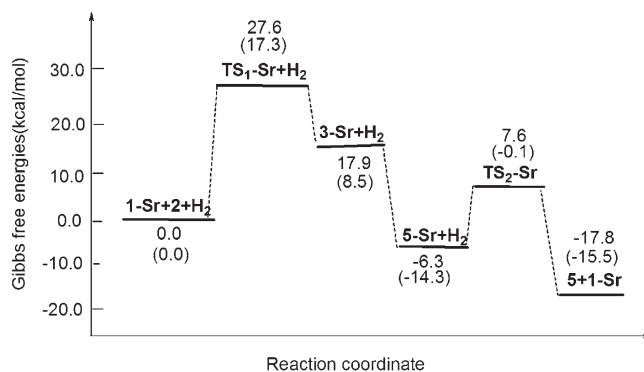


**Figure 6.** Gibbs free energy profile of the strontium-mediated hydrogenation reaction of DPE with  $H_2$  in the solvent. The corresponding free energies in the gas phase (60 °C and 20 bar) are also presented in parentheses for comparison.

the homoleptic dibenzylcalcium catalyst indeed exhibits similar catalytic activity as its strontium analog in alkene hydrogenation.<sup>39</sup>

#### 4. Conclusions

We have performed detailed theoretical calculations to investigate the molecular mechanism of the hydrogenation reactions of 1,1-diphenylethylene and myrcene catalyzed by the actual calcium hydride catalyst,  $CaH(dipp-nacnac)(thf)$ . The hydrogenation reactions of these two alkenes proceed via a similar pathway, which includes three steps. First, the hydride migrates from the calcium center to the terminal carbon of the double bond in the substrate to form the ion-pair intermediate. Then, the transient hydride transfer product could easily transform into the key ion-pair intermediate. In this key intermediate, the metal cation is bound to the negatively charged phenyl ring for 1,1-diphenylethylene, or one carbon atom of the allyl group for myrcene. This intermediate provides an intramolecular frustrated Lewis pair, in which the calcium center acts as a Lewis acid, and one olefinic carbon acts as a Lewis base. Next, the H–H bond is heterolytically cleaved by this frustrated Lewis pair through a concerted Lewis acid–Lewis base mechanism, producing the hydrogenation product and regenerating the catalyst. For these two reactions, the rate-limiting step is the hydride transfer step, with free energy barriers of 29.2 kcal for both substrates. The results can give satisfactory descriptions on experimental facts observed for these two hydrogenation reactions. According to this mechanism, the phenyl ring (for 1,1-diphenylethylene) and the conjugated double bond (for myrcene) are essential for the binding of the main-group metal to the substrate to form the key ion-pair intermediate, which acts as an intramolecular frustrated Lewis pair. In addition, the hydrogenation reactions of 1,1-diphenylethylene catalyzed by the analogous magnesium and strontium hydride complexes have also been studied. Our calculations indicate that the strontium-mediated hydrogenation reaction of 1,1-diphenylethylene may readily occur, but a similar magnesium-mediated hydrogenation reaction is less likely to take place under similar conditions as adopted by the calcium hydride catalyst.

It is worthwhile mentioning that the hydrogenation mechanism proposed here is different from that of the late transition metal-catalyzed alkene hydrogenation or the organolanthanide-catalyzed alkene hydrogenation.

The mechanism proposed here is somewhat similar to that of metal-free hydrogenation of imines, which are both based on heterolytic cleavage of H<sub>2</sub> by frustrated Lewis pairs. However, the detailed pathways are also different. In the present mechanism, the hydride first transfers from the catalyst to the substrate, and then the H–H bond is heterolytically cleaved by a frustrated Lewis pair to produce the product and regenerate the catalyst. While in the metal-free hydrogenation of imines, dihydrogen is first activated by the catalyst to produce a hydride and a proton. Then, the resulting hydride and the proton may transfer to the C–N bond of substrates in a stepwise manner to produce the product. We hope that the mechanistic insight revealed here

for the hydrogenation of alkenes with H<sub>2</sub> will be helpful for experimentalists to design more effective main-group metal-based catalysts for alkene hydrogenations.

**Acknowledgment.** This work was supported by the National Natural Science Foundation of China (Grant Nos. 20625309 and 20833003) and the National Basic Research Program (Grant No. 2004CB719901).

**Supporting Information Available:** Electronic energies, Gibbs free energies, and Cartesian coordinates of all stationary points. This material is available free of charge via the Internet at <http://pubs.acs.org>.